Journal of Computer Security and Data Forensics

Volume **1**, Number **1**, March **2021**

Overview of reversible data hiding

Tiancong Zhang[1], Shaowei Weng[1,*], Shu-Chuan Chu[2]

[1]School of Electronic, Electrical Engineering and Physics,
Fujian University of Technology,
Fuzhou, 350118, China

[2]College of Science and Engineering,
Flinders University,
Sturt Rd, Bedford Park SA 5042, Australia

Received January 2021; revised March 2021
(Communicated by: wswweiwei@126.com)

Abstract. *Reversible data hiding (abbreviated as RDH), also called as lossless or erasable data hiding, has experienced more than 20 years of development, from a capacity of only hundreds of bits to a capacity of exceeding 1 bpp (bit per pixel), from traditional spatial domain to compressed domain (e.g., vector quantization, joint photographic experts group), from natural images to encrypted images, from images to videos or audios, from fragile authentication to semi-fragile (or robust) RDH, etc.. During these two decades, a considerable amount of attention has been devoted to study RDH, and more and more papers in various research branches of RDH have been published. In this paper, we will give a detailed introduction on RDH from the following five aspects: 1) RDH in the traditional spatial domain; 2) RDH in the compressed domain; 3) RDH for encrypted images; 4) semi-fragile authentication RDH; 5) video and audio RDH.*
Keywords: RDH, High capacity, Image encryption, Image recovery, Video RDH, Audio RDH, RDH in the spatial domain, RDH the compressed domain, RDH for encrypted images, Semi-fragile authentication, Robust

1. **Introduction.** Data hiding is a technique that hides data imperceptibly into a cover carrier, and enables the hidden data to be extracted from the stego carrier for various purposes such as copyright protection, image authentication. However, most data hiding algorithms cause permanent distortion to the cover carrier when embedding data, and hence cannot ensure lossless recovery of the original carrier. Such permanent distortion is unacceptable for some quality sensitive applications, such as medical imaging, where the complete recovery of the original carrier is required. Reversible data hiding (RDH) is exactly the technique that can solve this problem because it has the advantage of accurately retrieving the original carrier even after the hidden data is correctly extracted [1].

RDH was firstly proposed by Barton in a US patent [2] in 1997 for image authentication. Since Barton performed lossless compression to leave space for accommodating the authentication information, the obtained capacity was relatively low. For a long time after the patent, lossless image compression algorithms had been used in early RDH methods to vacate space for embedding data [3–6]. Until the publication of Tian's method [7, 8], the embedding capacity reaching close to 0.5 bpp (bit per pixel) was achieved. Tian proposed difference expansion (DE) to embed one bit of data into two adjacent pixels (i.e., a pixel pair). In 2004, Alattar proposed a generalized integer transform (GIT) to extend DE from two adjacent pixels to n consecutive pixels ($n > 2$) [9]. As a result, the maximum

embedding capacity was increased from 0.5 bpp to $1 - 1/n$ bpp. Considering that a large distortion must occur when expanding a large difference using DE, Zhang *et al.* proposed a histogram shifting (HS)-based RDH method in 2003 [10]. HS conceals one bit of data into the peak pixel having the largest occurrence frequency while shifting other pixels by 1 for reversibility. HS can produce a relatively high visual quality ($\geq$ 48.13 dB) because it modifies slightly pixels to embed data into an image. However, the embedding capacity is low and limited by the peak height. For Tian's method and Alattar's method, from the perspective of prediction, the difference is generated by simply predicting each pixel using its adjacent pixel, and thus, the difference histogram is not sharp. In 2007, Thodi *et al.* introduced the median edge detector (MED [11]) into RDH to predict each pixel using its three neighbors such that a sharp prediction error histogram (PEH) was obtained [12]. The DE, HS, prediction error expansion (PEE) and integer transform (IT) are the four fundamental works of RDH, and various skills have been introduced into these works to improve the performance [13–17].

Compared with uncompressed images, the compressed images that require less storage space and transmission time are widely used in our life. In addition to hiding data into an uncompressed image by modifying pixel values, the compressed domain RDH methods (another branch of RDH) have already been explored to change the coefficients of the compressed codes for embedding data. Correspondingly, many related RDH methods in various compression formats have bee proposed, such as VQ [18–25], JPEG [26–41], and AMBTC (Absolute Moment Block Truncation Coding) [42–48]. Note that the compressed domain RDH methods cannot offer the same embedding capacity as the spatial domain RDH methods because the redundancy of a compressed image is considerably eliminated.

For reducing the calculation burden and saving storage space on user client, a large number of personal data are stored or processed on the cloud storage platform. However, the content owner might not want other person, e.g., cloud server (data hider), to know the principal image contents before embedding data. Therefore, the content owner has to encrypt image contents before sending them to data hider, and then, data hider embeds data into encrypted images for privacy protection. The adopted data hiding method capable of retrieving exactly the original image content after decryption is called RDH in encrypted images (RDHEI). RDHEI has been extensively studied in recent years, and many works about RDHEI have bee proposed [49–62].

Most of RDH methods are fragile, in which the hidden data cannot be recovered completely even if the stego image suffers very slight degradation (e.g., JPEG compression or noise addition). De Vleeschouwer *et al.*'s histogram rotation (HR) has been deemed to be the first robust (or semi-fragile) RDH against high-quality JPEG compression [63, 64]. Afterwards, some robust RDH methods have been proposed to achieve good robustness [65–72].

A digital image is often used as a message carrier in many data hiding techniques. The halftone image is a special kind of image, which is generated by converting a continuous-tone image (e.g., an 8-bit grayscale image) into a two-tone image (e.g., a binary image). The research on RDH for halftone images has been carried out in recent years [73–75]. Besides images, other existing digital media such as audio, video can also be served as the carrier. Some investigations on video/audio RDH have been conducted to improve the embedding performance, and many related papers have been proposed [76–89].

After having the basic concepts and main research branches of RDH, the rest of the paper is organized as follows. A summary of existing spatial domain RDH methods is presented and analyzed in Section 2. In the next section, a comprehensive introduction for the compressed domain RDH methods is given. Besides JPEG, both VQ and AMBTC are combined into this section. Section 4 describes three main branches of RDHEI. Section 5

introduces the robust (or semi-fragile) RDH. In Section 6, besides images, RDH can be used to video or audio RDH. Section 7 summarizes the results of this investigation.

2. **RDH in spatial domain.** RDH in the spatial domain has been developed greatly since it originally appeared in Barton's patent. According to whether the optimal selection strategy is used to preferentially select the pixels located in smooth regions or not, the RDH methods in the spatial domain are partitioned into two main types: high-capacity RDH and high fidelity RDH. We will introduce these two types separately in the following two subsections.

2.1. **High-capacity RDH.** The early RDH methods, including lossless compression, DE, HS, IT, and PEE, are categorized into the 1^{st} type. This is because these methods processed indifferently the pixels located in the smooth and complex regions. Next, we will introduce these methods one by one.

2.1.1. *DE.* DE refers to the embedding process summarized in Eq. (1), in which the difference d between two adjacent pixels x and y is doubled such that the LSB (Least Significant Bit) of d' is vacated for embedding 1-bit data, where d' is the stego value of d.

$$d' = d \times 2 + b_1, \tag{1}$$

where b_1 is one bit of data to be embedded.

The average value h of x and y remains unaltered before and after data embedding, i.e., $h = \lfloor (x' + y')/2 \rfloor = \lfloor (x + y)/2 \rfloor$, such that the reversibility is effectively ensured, where x' and y' are the stego pixels of x and y, respectively, and they are obtained by the inverse transform of the Haar IT in Eq. (2).

$$\begin{aligned} x' &= h + \left\lfloor \tfrac{d'+1}{2} \right\rfloor, \\ y' &= h - \left\lfloor \tfrac{d'}{2} \right\rfloor. \end{aligned} \tag{2}$$

In Tian's method, some stego pixels (e.g., x' or y') may exceed the pixel value range (e.g., [0,255] for an 8-bit grayscale image), and thus, for reversibility, their corresponding original pixels must be excluded from embedding data. To identify these unused pixels during data extraction, a location map that is a binary matrix needs to be created to record their locations. For blind data extraction and image recovery, this map is embedded along with the payload into the cover image. Usually, to save embedding space, it must be compressed losslessly before embedding. However, the compressed map still occupies a large portion of the embedding space.

2.1.2. *Alattar's method.* The GIT defined in Eq. (3 is applied to n pixels of an image block to create $n-1$ difference values $(v_1, v_2, \cdots, v_{n-1})$ and one average value v_0. The average value v_0 is used to maintain reversibility while each of $n-1$ difference values is expanded to carry one bit of data.

$$\begin{aligned} v_0 &= \left\lfloor \tfrac{x_1 + x_2 + \cdots + x_n}{n} \right\rfloor, \\ \tilde{v}_1 &= 2(x_2 - x_1) + b_1 = 2v_1 + b_1, \\ \tilde{v}_2 &= 2(x_3 - x_1) + b_2 = 2v_2 + b_2, \\ &\vdots \\ \tilde{v}_{n-1} &= 2(x_n - x_1) + b_{n-1} = 2v_n + b_{n-1}. \end{aligned} \tag{3}$$

where x_1, $x_2, \cdots, x_n$ were n pixels of an image block.

The inverse transform of GIT was formulated below:

$$\begin{aligned} y_1 &= v_0 - \left\lfloor \frac{\tilde{v}_1+\tilde{v}_2+\cdots+\tilde{v}_{n-1}}{n} \right\rfloor, \\ y_2 &= \tilde{v}_1 + v_0 - \left\lfloor \frac{\tilde{v}_1+\tilde{v}_2+\cdots+\tilde{v}_n}{n} \right\rfloor, \\ &\vdots \\ y_n &= \tilde{v}_{n-1} + v_0 - \left\lfloor \frac{\tilde{v}_1+\tilde{v}_2+\cdots+\tilde{v}_n}{n} \right\rfloor. \end{aligned} \tag{4}$$

where y_i is used to denote the stego pixel value, where $i \in \{1, \cdots, n\}$.

Similar to Tian's method, Alattar's method also needs a location map to record the locations of blocks containing overflowed or underflowed pixels.

2.1.3. *Weng* et al.*'s method.* To reduce the size of the compressed map, Weng *et al.* proposed an integer transform that could maintain the sum of two neighboring pixels invariant [90] in 2008. The integer transform is summarized below:

$$\begin{aligned} x' &= x + M(d), \\ y' &= y - M(d), \end{aligned} \tag{5}$$

where $M(d)$ that represents the pairwise difference adjustment (PCA) technique is defined as:

$$M(d) = \begin{cases} \left\lfloor \frac{d}{2} \right\rfloor + b, & \text{if } |d| < T_h, \\ \text{sign}(d) \times C_0, & \text{if } |d| \geq T_h, \end{cases} \tag{6}$$

where T_h is a predefined threshold, which is used to achieve a satisfactory balance of the distortion and embedding capacity, $\text{sign}(d)$ is 1 if $d \geq 0$; otherwise, $\text{sign}(d) = -1$, C_0 is a constant equal to $\lfloor (T_h + 1)/2 \rfloor$.

For the pixels larger than or equal to T_h, if they are directly expanded to embed data, the distortion is unacceptable, leading to a serious decrease in visual quality. PDA enables these pixels to be shifted by C_0 such that the embedding distortion is effectively decreased, and meanwhile, the number of pixels causing overflows or underflow is reduced, directly resulting in a severe reduction in the size of the compressed map.

Afterwards, Wang *et al.* reformulated DE as an IT and extended this transform from two neighboring pixels to n consecutive pixels [91, 92]. Peng *et al.* performed adaptive data embedding according to the image block type determined by the pre-estimated distortion [93]. Weng *et al.* utilized the invariant average value of GIT to evaluate the smoothness of each image block, and priorly selected the blocks in smooth regions for embedding, and therefore, the embedding performance was improved [94].

2.1.4. *HS.* As illustrated in Figure 1, the cover pixel having the highest occurrence frequency is called the peak point while the cover pixel with the lowest occurrence frequency is called the zero point. The pixels located between the peak point and the zero point are shifted outwards by 1 to leave space for the peak point such that the peak point can embed one bit of data for reversibility. In a word, one pixel is modified by 1 at most, so HS can maintain satisfactory visual quality.

2.1.5. *PEE.* Referring to Eq. (7), the predictor MED is used to predict each pixel using its three neighboring pixels (see Figure 2 for details), rather than one pixel like in Tian's method and Alattar's method, so the predicted value $\tilde{x}$ is closer to x, and the prediction error e becomes smaller, where $e = x - \tilde{x}$.

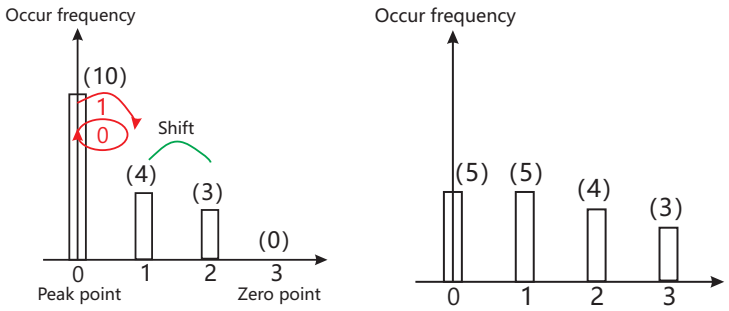

(a) Before HS (b) After HS

FIGURE 1. A simple example of HS.

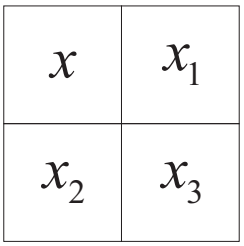

FIGURE 2. x represents the current pixel, and x_1, x_2, x_3 constitute the neighborhood of the pixel x.

$$\tilde{x} = \begin{cases} \min(x_1, x_2), & \text{if } x_3 \geq \max(x_1, x_2), \\ \max(x_1, x_2), & \text{if } x_3 \leq \min(x_1, x_2), \\ x_1 + x_2 - x_3, & \text{otherwise.} \end{cases} \tag{7}$$

In Thodi *et al.*'s method, the prediction error e is modified via Eq. (8) to generate its stego value e'.

$$e' = \begin{cases} 2e + b, & \text{if } e \in [-T_h, T_h), \\ e + T_h, & \text{if } e \geq T_h, \\ e - T_h, & \text{if } e < -T_h. \end{cases} \tag{8}$$

Finally, the stego pixel $x' = x + e'$. By means of PEE and HS, Thodi *et al.* could provide high embedding capacity of close to 1 bpp while maintaining low distortion.

Later on, the PEE technique has been investigated extensively and developed rapidly, and some research papers have been reported in the literature. According to the way that the predictor is designed, the research papers can be classified into two classes [95].

For the first class, the predictor is designed using the casual context of the current pixel [13, 16, 96, 97]. Sachnev *et al.* proposed an RDH method combining the rhombus predictor and sorting [13]. Figure 3 depicts that the current pixel x is predicted by its four pixels surrounding it, and the predicted value $\tilde{x} = \lfloor (x_1 + x_2 + x_3 + x_4)/2 \rfloor$. Since the rhombus predictor utilizes four nearest neighbor pixels to predict the current pixel, a sharper histogram is generated. The sorting technique is employed to select priorly the pixels in smooth regions for embedding. In 2011, Li *et al.* proposed a RDH method based on adaptive PEE and block selection [98]. The gradient-adjusted prediction (Gap) is used to predict each pixel using the prediction context containing seven neighbors, rather than three neighbors in MED. One smooth pixel is expanded twice to carry two bits while one

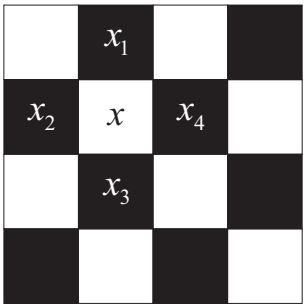

FIGURE 3. The rhombus predictor.

rough pixel is expanded once to carry one bit, obtaining a better performance for high payloads.

The second class is to generate the predictor by utilizing the image interpolation mechanism [15,99–103]. Among them, Luo *et al.* utilized an interpolation technique to generate interpolation errors, and expanded additively one interpolation error for embedding bit '1' or '0'. Due to the slight modification of pixels, Luo *et al.* could achieve a large payload while maintaining high visual quality [15].

2.2. **High fidelity RDH.** High fidelity RDH performs well for low payload ($<$ 0.1 - 0.2 bpp) by selecting preferentially the pixels located in smooth regions for embedding data while excluding the pixels in highly-textured regions from embedding data [16, 104–123].

Li *et al.* proposed a predictor based on pixel-value-ordering (PVO), which split an original image into non-overlapping image blocks, and then measured the local complexity of one block to distinguish whether this block was smooth ($\Delta \leq T_h$) or complex ($\Delta > T_h$) [16], where the notation Δ was used to denote the local complexity. For a smooth block, PVO is used to predict the maximum using the second largest pixel and the minimum using the second smallest pixel. The maximum is additively embedded with one bit or increased by 1. Similarly, the minimum is additively embedded with one bit or decreased by 1. Since two pixels at most in a smooth block are modified, and each pixel is modified by 1 at most, Li *et al.*'s method can offer satisfactory visual quality at low payload. However, Li *et al.*'s method still has the following two disadvantages: 1) the prediction error equal to 0 is excluded from embedding data; 2) each block is embedded with two bits at most. To solve these two problems, some improved versions of PVO have been proposed, such as PVO-k [104], PPVO (pixel-based PVO) [105, 106], IPVO (Improved PVO) [107, 108]. Weng *et al.* proposed an adaptive pixel modification strategy, in which the smoother one block was, the more the pixels involved in data embedding were, and the more the bits that were hidden into this block were, and vice verse [109, 110]. Wang *et al.* proposed a dynamic block modification strategy to split flat areas into smaller blocks and complex areas into larger blocks, and utilized PVO to modify the maximum and minimum pixels in each block for embedding data [111]. Weng *et al.* improved Wang *et al.*'s method to divide the cover image into blocks of arbitrary length [112].

For the case of low payload, the P-PEE (pairwise PEE) proposed by Ou *et al.* is also an efficient scheme. In P-PEE, every two adjacent prediction errors is treated as a prediction-error pair [113]. To decrease the distortion, a pair valued (0,0) can be additively embedded with $log_2 3$ bits, rather than 2 bits (i.e., the combinations of two bits, '00', '01', '10' and '11'), by preventing the last combination '11' from being embedded into the pair. Dragoi and Coltuc introduced adaptive pairing, rather than fixed paring like in Ou *et al.*'s method [113], increasing the number of embeddable pairs and decreasing the number of shifted pixels [114]. In 2019, Ou *et al.* improved P-PEE by proposing adaptive

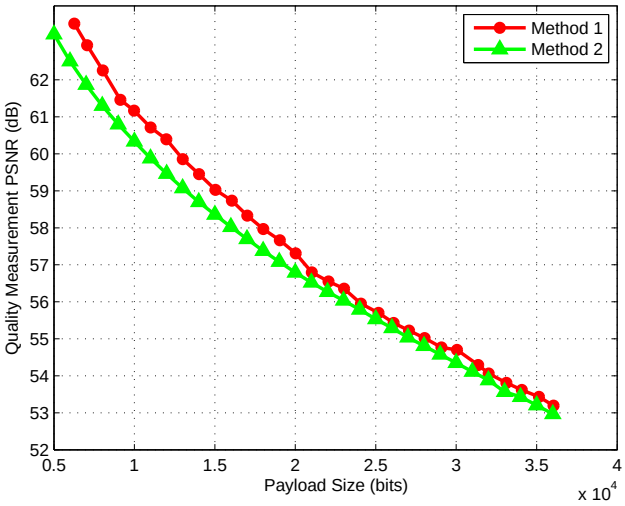

FIGURE 4. Capacity-distortion curve for RDH.

pixel pairing (APP) and adaptive mapping selection [115]. In addition, some scholars have proposed RDH schemes in combination with PVO and P-PEE [116, 117]. Xiao *et al.* proposed the optimal expansion path with the adaptive embedding mechanism for enhancing the embedding performance [118].

Li *et al.* designed a new embedding mechanism called multiple histogram modification (MHM) for multiple sub-histograms [119]. As illustrated in Figure 5, the prediction-error histogram is divided into multiple sub-histograms. Two expansion bins are selected in each sub-histogram, and data embedding is performed according to MHM. Wang *et al.* selected FCM (Fuzzy C-means) equipped with deliberately designed features to construct multiple sub-histograms [120]. Weng *et al.* utilized the K-means cluster algorithm to construct multiple sub-histograms according to the local complexity, and introduced the improved crisscross optimization algorithm to search for the approximate optimal [123]

2.3. **Image quality measure metrics.** As has been pointed out in [124], the visual quality of stego images and the embedding capacity are two quality measure metrics that are applied most frequently in data hiding to evaluate the capacity-distortion performance. Figure 4 indicates that a tradeoff between the two metrics exists because the embedding capacity is increased at the cost of image distortion, and vice versa.

PSNR is used most commonly to measure the visual quality of stego images. However, PSNR does not always predict the perceptual image quality. In fact, improving the perceptual visual quality such as contrast enhancement is more important than just obtaining high PSNR, especially for illuminated images. Wu *et al.* incorporated HS into histogram equalization (a popular contrast enhancement method) to achieve both data embedding and contrast enhancement [125–127]. Specifically, the highest two bins (peaks) that are located on the left and right sides of the histogram, respectively, are selected. Next, the bins between the two peaks remain unaltered while other bins are shifted outwardly to vacate the bin next to each peak for embedding data. The process is carried out recursively until the required embedding capacity and high contrast enhancement are achieved. Afterwards, RDH with contrast enhancement (RDH-CE) has been widely investigated, and some related works have been proposed [124, 128–131].

3. **RDH in the compressed domain.** Digital images are usually compressed to reduce the bit rate for transmission or storage in real applications, that is, images are often

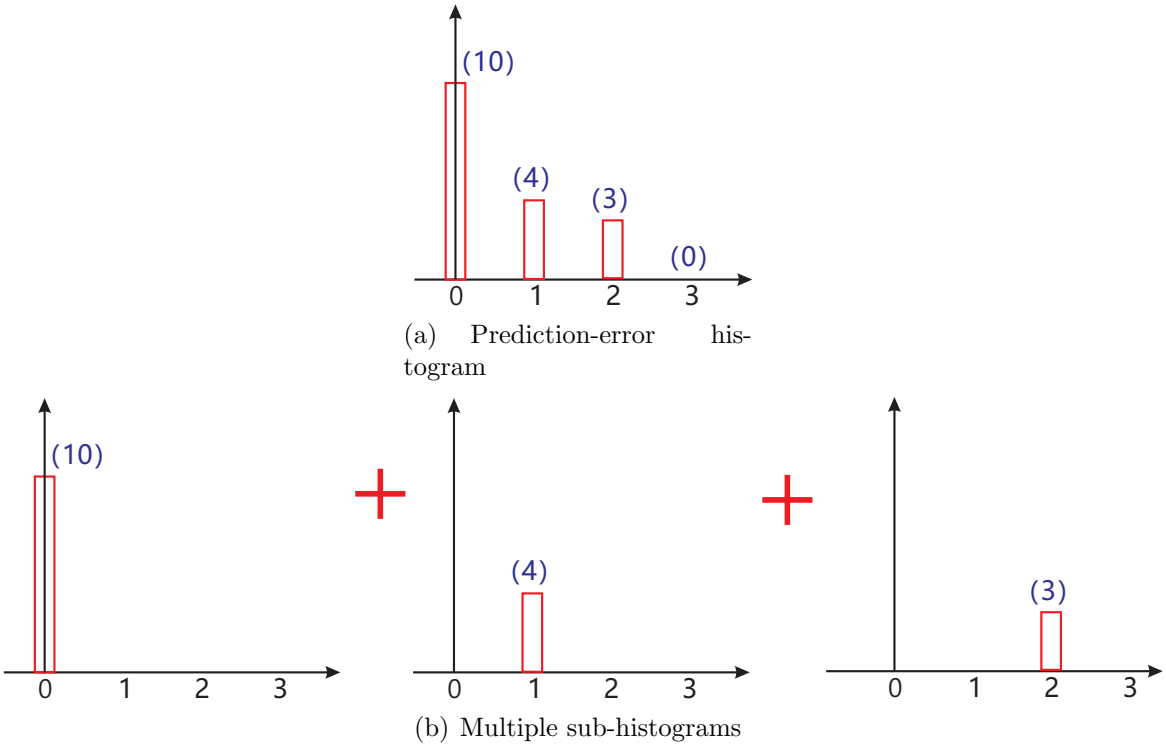

FIGURE 5. A simple example of multiple sub-histograms.

transmitted and stored in the compressed format. The compressed domain RDH method refers to the method that embeds data into the compressed codes generated by compressing and encoding an image. The compressed domain RDH methods have attracted the attention of many scholars, and have obtained the rich research results which are classified mainly into three types: 1) VQ, 2) JPEG, 3) absolute moment block truncation coding (AMBTC).

3.1. **RDH for VQ images.** VQ is a commonly-used lossy compression method that is capable of significantly reduce the file size while maintaining acceptable visual quality. To compress a cover image using VQ, this image is firstly split into equal-sized non-overlapping blocks, and then each block is denoted by the index of the codeword having the minimum Euclidean distance to this block. Two metrics that are used to estimate the performance of a RDH method for VQ images are the bitrate and embedding rate. The bitrate refers to the ratio of the length of the stego code stream to the number of pixels in an image. A smaller bitrate implies that the stego code stream requires less storage space and takes less transmission time. The embedding rate is used to determine the number of bits embedded into each VQ index. A larger embedding rate indicating a higher embedding capacity is what we want. Reducing the bitrate as much as possible while maintaining a satisfactory embedding rate has been attracting researchers to explore new research techniques.

The existing RDH methods for VQ images can be classified into two groups [25]. RDH methods in Group 1 have the characteristic that the retrieved indices during data extraction can be directly decoded by the standard VQ decoder, but cannot provide high embedding capacity [20]. In contrast, RDH methods in Group 2 rearrange indices using the neighboring coding technique such that high embedding capacity can be achieved [19, 21, 22, 24, 25]. Note that a map between the original indices and rearranged indices needs to be transmitted to receivers to reconstruct the original indices.

Compared with Group 1, Group 2 can provide higher payloads, and hence, has received more attention from researchers in recent years. As a recently-published paper of Group 2, Hong *et al.* exploited the AIA (adaptive indicator assignment) technique to generate a compressible RI (rearranged indices) that was advantageous for prediction coding, improved prediction performance using the LSE (least square estimator) technique, and finally utilized the dual coding modes (DCM) to reduce effectively the length of the output code bitstream [25]. By means of the three techniques, Hong *et al.*'s method offered a reduced bitrate and achieved a comparable payload.

3.2. **RDH for JPEG images.** JPEG is a widely-used lossly compression method that can offer high compression rates while keeping acceptable visual quality. The JPEG encoder is mainly composed of three steps: two-dimensional discrete cosine transform (2D DCT), a quantizer, and a JPEG entropy encoder. 2D DCT is firstly applied to each 8×8-sized non-overlapping block to get the corresponding 64 DCT coefficients. Next, the quantizer containing 8×8-sized predetermined quantization table is employed to quantize each coefficient. Finally, the quantized coefficients are encoded using the JPEG entropy encoder to form the output bitstream. Specifically, the JPEG entropy encoder scans sequentially 64 quantized coefficients according to the zigzag order to get a coefficient list. The direct current (DC) coefficient is encoded using the differential pulse code modulation (DPCM) while each of the remaining coefficients is encoded using length encoding (RLE). The encoded bitstream is Huffman coded to obtain the output bitstream.

Similar to RDH for uncompressed images, RDH for JPEG images can also be classified into two types: RDH for JPEG images [26–39] and RDH for encrypted JPEG images [40, 41].

In terms of embedding strategies, the existing RDH methods for JPEG images can be summarized into four categories: lossless compression [26, 27], quantization table and quantized DCT coefficients [35], Huffman table [28, 32–34], quantized DCT coefficient [30, 31, 37–39]. Type-I method achieve data embedding by compressing the LSB plane of some selected JPEG coefficients [26, 27]. Since the redundancies of a JPEG image are eliminated, Type-I methods can provide very limited embedding capacity. In addition, Type-I methods easily cause low visual quality and increase the file size of a stego JPEG image. Type-II methods create space for embedding data by modifying the quantization table and quantized DCT coefficients [35]. Type-II methods can achieve high embedding capacity and provide high visual quality. However, these methods cause a significant increase in file size because they break the tradeoff between the file size and the visual quality by changing the quantization table. Type-III methods can preserve the file size of a stego JPEG image while maintaining satisfactory visual quality. However, their embedding capacity is relatively low. Specifically, only hundreds of bits are embedded into a cover image with size of 512×512. Type-VI methods achieve data embedding by modifying the DCT coefficients while preserving the quantization table. Type-VI methods can achieve both high embedding capacity and good visual quality while preserving well the storage size of a stego JPEG image. Therefore, Type-VI methods have gradually become a hot research topic, and attracted extensive attention from scholars. Chang *et al.* utilized two successive mid-frequency DCT coefficients valued 0 in each block for embedding data [30]. Xu *et al.* designed an optimal search strategy to select low-frequency and mid-frequency DCT coefficients and shifted the histogram of the selected coefficients for embedding data [31]. Huang *et al.* sorted 4098 8×8-sized blocks according to the number of zero coefficients in each block, and selected priorly the blocks with more zero

coefficients for embedding [37]. To preserve the file size, the coefficients valued 1 or -1 in one block are embedded with data while the zero coefficients remain unchanged. Recently, Huang *et al.* proposed the pairwise nonzero AC coefficient expansion (NACE) to generate a sharp two-dimensional histogram [38]. He *et al.* selected the frequencies with small negative indices for carrying data with a high prior by designing the image visual distortion model and file size change model [39].

3.3. **RDH for AMBTC-compressed images.** The AMPTC compressed method that was proposed by Mitchell in 1984 [132] achieves compression by representing an image block using an AMBTC trio. Each trio is composed of two quantization levels and a bitmap. Taking the i^{th} image block I_i of size $r \times c$ for example, suppose a_i is used to denote the mean value of I_i, and the AMBTC trio is (l_i, s_i, B_i), where the upper quantization level l_i is used to represent the average value of pixels larger than or equal to a_i, the lower quantization level s_i indicates the average value of pixels smaller than a_i, the bitmap B_i of the same size as I_i is generated to distinguish which elements of I_i correspond to l_i and which pixels correspond to s_i. If $I_{i,j} \leq a_i$, $B_{i,j} = 1$; otherwise, $B_{i,j} = 0$, where $I_{i,j}$ is used to denote the j^{th} pixel of I_i.

On the decoding stage, after obtaining an AMBTC trio (l_i, s_i, B_i), the bits of B_i are scanned sequentially. If $B_{i,j} = 1$, then $C_{i,j} = l_i$; otherwise, $C_{i,j} = s_i$, where $C_{i,j}$ is used to denote the j^{th} pixel of the block C_i that is reconstructed from the trio (l_i, s_i, B_i). It is interesting to note that the reconstructed block C_i is not the same as the cover image $I_{i,j}$, and therefore, AMPTC is a lossly compression method.

According to the description mentioned above, AMBTC requires insignificant calculation cost and offers satisfactory visual quality. Many studies have been devoted to investigating RDH for AMBTC compressed codes, which can retrieve losslessly the AMBTC compressed image after the embedded data are correctly extracted [42–48]. Similar to VQ, all the works can be classified into two classes according to whether the stego AMBTC compressed image can be decoded by the standard AMBTC decoder or not [48]. A special decoder, rather than the standard decoder used in Type 1, is need for Type 2 [45–47]. Furthermore, the stego AMBTC compressed codes of Type 2 have a different length with the conventional AMBTC codes, increasing the risks of being perceived and attacked by attackers. Thus, Type 2 has weak security.

4. **RDH in Encrypted images.** Recently, many studies have been performed to improve the performance of RDHEI, and some works have been presented [49–57, 59–61]. The RDHEI methods have been developed in the following three main branches: VRAE (vacating data-hiding room after encryption) [49–54], RRBE (reserving data-hiding room before encryption) [55–59] and homomorphic cryptosystems which can perform data embedding in encrypted domain [60, 61].

In fact, the first branch has more practical applications than the second branch because it do not require additional pre-processing before encryption, while increased the computational burden of the content owner. However, the first branch may seriously degrade the visual quality of the decrypted, stego images. The second branch can acquire more payload than the first branch because it reserves data-hiding room before encryption. The third branch easily increased computational complexity.

5. **Robust (or semi-fragile authentication).** Robust (or semi-fragile authentication) RDH (RRDH) can allow the exact recovery of the cover image and the complete extraction of hidden data in case of no attack. Conversely, the hidden data need to be robust against unintentional attacks (e.g., JPEG compression and addition noise), that is, the hidden data can still be extracted completely even if the stego image is distorted by unintentional

attacks. In this case, the distorted stego image cannot be reversed to its original state. Studying RRDH may enlarge the applicable scope of RDH because it enables RDH to transmit data in a lossy environment [66]. However, RRDH has received insignificant attention in the literature, and only a few works have been presented [65–72].

De Vleeschouwer *et al.* ware the first to propose an RRDH method (namely HR) robust against JPEG compression, the key idea of which was to partition randomly an image block into two equal-sized sets, and modified the centroid vectors of two sets for embedding data. Afterwards, Ni *et al.* proposed an improved version of De Vleeschouwer *et al.*'s method to solve the salt-and-pepper noise of HR [65]. In addition, Ni *et al.* introduced the error correction coding (ECC) to correct error bits on the decoder side for the blocks containing overflowed or underflowed pixels, directly leading to a low embedding capacity. Zeng *et al.* embedded bits into blocks by shifting the histogram produced by the arithmetic value of each block [66]. Gao *et al.* improved Zeng *et al.*'s method by incorporating the merits from the generalized statistical quantity histogram (GSQH) and the histogram-based embedding [67]. Thereafter, An *et al.* proposed a novel pragmatic framework called WSQH-S (wavelet-domain statistical quantity HS and clustering), in which the histogram was produced using the coefficients of the wavelet-transformed image [68]. An *et al.* an RRDH method in combination with statistical quantity histogram shifting and clustering [69]. An *et al.* improved the HR-based embedding model of De Vleeschouwer *et al.* [70]. Thabit *et al.* proposed a novel RRDH using Slantlet transform matrix, which embedded the watermark bits by modifying the mean values of the carrier subbands [71]. Recently, inspired by [133, 134], Wang *et al.* proposed an independent embedding domain (ED) based two-stage RRDH [72].

6. **Video and audio RDH.** In this section, we will introduce separably the video and audio RDH in the following two subsections.

6.1. **Video RDH.** Some video coding standards such as MPEG-2/4, H.264/AVC and high efficiency video coding, have been proposed to compress and code video signals for transmitting video over bandwidth-limited channels. Considering that H.264/AVC is one of the most commonly used video coding standards, the research on RDH for H.264/AVC videos has attracted more and more attention from scholars. The existing RDH methods for H.264/AVC videos can be divided into two main branches according to the modification strategies: motion vector [76, 77] and quantized DCT coefficients [78–81].

To avoid privacy leakage, video bitstreams have to be encrypted before being uploading to the cloud server. Therefore, the RDH methods for encrypted H.264/AVC also have been extensively studied in recent years [82, 83].

6.2. **Audio RDH.** Similar to digital images, digital audio is also one of the main media that is delivered widely over the internet. The RDH techniques that have been proposed for images, such as PEE, HS, DE, can also be applied into audio. Similar to digital images, according to the applied domain, audio RDH can be classified into three categories: spatial domain [84–87], transformed domain [88] and compressed domain [89].

7. **Conclusions.** Shi *et al.* gave a comprehensive overview of the existing RDH techniques in 2016 [135]. There are three main differences between Shi *et al.*'s paper and ours. The first one is that we classified RDHCE into the spatial domain RDH methods. Secondly, RDH methods in the compressed domain included the RDH methods of three compression formats: VQ, AMBTC, and JPEG. Finally, we introduced some recently-published papers (especially published after 2016) into our reference list. In this paper, we gave a detailed introduction for five research branches of RDH: the spatial domain

RDH, the compressed domain RDH, RDHEI, semi-fragile RDH (or robust) RDH, and video or audio RDH.

8. **Acknowledgements.** This work was supported in part by the National NSF of China under Grant 61872095, Grant 61571139, Grant 61872128, in part International Scientific and Technological Cooperation of Guangdong Province under Grant 2019A050513012, in part by the Open Project Program of Shenzhen Key Laboratory of Media Security under Grant ML-2018-03, in part by Fujian Science Fund for Distinguished Young Scholars under Grant 2020J06043.

REFERENCES

[1] H. C. Huang, Y. H. Huang, J. S. Pan, and Y. Y. Lu, "Information protection and recovery with reversible data hiding," in *International Conference on Intelligent Information Hiding and Multimedia Signal Processing*, 2007, pp. 461–464.

[2] J. Barton, *Method and Apparatus for Embedding Authentication Information withinData.* US patent:5646997, 1997.

[3] M. U. Celik, G. Sharma, A. M. Tekalp, and E. Saber, "Lossless generalized-LSB data embedding," *IEEE Trans. Image Process.*, vol. 14, pp. 253–266, 2005.

[4] M. U. Celik, G. Sharma, and A. M. Tekalp, "Lossless watermarking for image authentication: a new framework and an implementation," *IEEE Trans. Image Process.*, vol. 15, pp. 1042–1049, 2006.

[5] J. Fridrich, M. Goljan, and R. Du, "Invertible authentication," in *SPIE Proceedings of Security and Watermarking of multimedia Content*, vol. 3971, San Jose, 2001, pp. 197–208.

[6] ——, "Lossless data embedding new paradigm in digital watermarking," *EURASIP J. Appl. Signal Process.*, vol. 2002, pp. 185–196, 2002.

[7] J. Tian, "Wavelet-based reversible watermarking for authentication," *Proc. SPIE*, vol. 4675, pp. 679–690, 2002.

[8] ——, "Reversible data embedding using a difference expansion," *IEEE Trans. Circuits Syst. Video Technol.*, vol. 13, no. 8, pp. 890–896, 2003.

[9] A. M. Alattar, "Reversible watermark using the difference expansion of a generalized integer transform," *IEEE Trans. Image Process.*, vol. 13, no. 8, pp. 1147–1156, 2004.

[10] Z. Ni, Y. Q. Shi, N. Ansari, and W. Su, "Reversible data hiding," *IEEE Trans. Circuits Syst. Video Technol.*, vol. 16, pp. 354–362, 2006.

[11] M. J. Weinberger, G. Seroussi, and G. Sapiro, "The LOCO-I lossless image compression algorithm: Principles and standardization into JPEG-LS," *IEEE Trans. Image Process.*, vol. 9, no. 8, pp. 1309–1324, 2000.

[12] D. M. Thodi and J. J. Rodríguez, "Expansion embedding techniques for reversible watermarking," *IEEE Trans. Image Process.*, vol. 16, no. 3, pp. 721–730, 2007.

[13] V. Sachnev, H. J. Kim, J. Nam, S. Suresh, and Y. Q. Shi, "Reversible watermarking algorithm using sorting and prediction," *IEEE Trans. Circuits Syst. Video Technol.*, vol. 19, no. 7, pp. 989–999, 2009.

[14] Y. J. Hu, H.-K. Lee, and J. W. Li, "DE-based reversible data hiding with improved overflow location map," *IEEE Trans. Circuits Syst. Video Technol.*, vol. 19, no. 2, pp. 250–260, 2009.

[15] L. Luo, Z. Chen, M. Chen, X. Zeng, and Z. Xiong, "Reversible image watermarking using interpolation technique," *IEEE Trans. Inf. Forensics Secur.*, vol. 5, no. 1, pp. 187–193, 2010.

[16] X. L. Li, J. Li, B. Li, and B. Yang, "High-fidelity reversible data hiding scheme based on pixel-value-ordering and prediction-error expansion," *Signal Process.*, vol. 93, no. 1, pp. 198–205, 2013.

[17] D. Coltuc, "Low distortion transform for reversible watermarking," *IEEE Trans. Image Process.*, vol. 21, no. 1, pp. 412–417, 2012.

[18] P. Tsai, "Histogram-based reversible data hiding for vector quantisation compressed images," *IET Image Process.*, vol. 3, no. 2, pp. 100–114, 2009.

[19] C. C. Chang, T. Kieu, and W. Wu, "A lossless data embedding technique by joint neighboring coding," *Pattern Recognit.*, vol. 42, no. 7, pp. 136–154, 2009.

[20] C. H. Yang, W. J. Wang, C. T. Huang, and S. J. Wang, "Reversible steganography based on side match and hit pattern for VQ-compressed images," *Inf. Sci.*, vol. 181, no. 11, pp. 2218–2230, 2011.

[21] J. X. Wang and Z. M. Lu, "A path optional lossless data hiding scheme based on VQ joint neighboring coding," *Inf. Sci.*, vol. 179, no. 19, pp. 3332–3348, 2009.

[22] J. D. Lee, Y. H. Chiou, and J. M. Guo, "Lossless data hiding for VQ indices based on neighboring correlation," *Inf. Sci.*, vol. 221, pp. 419–438, 2013.
[23] C. C. Lin, X. Liu, and S. Yuan, "Reversible data hiding for VQ-compressed images based on search-order coding and state-codebook mapping," *Inf. Sci.*, vol. 293, pp. 314–326, 2015.
[24] D. Kieu and A. Rudder, "A reversible steganographic scheme for VQ indices based on joint neighboring and predictive coding," *Multimed. Tools Appl.*, vol. 75, no. 21, pp. 13 705–13 731, 2016.
[25] W. Hong, X. Y. Zhou, D.-C. Lou, T. S. Chen, and Y. Y. Li, "Joint image coding and lossless data hiding in VQ indices using adaptive coding techniques," *Inf. Sci.*, vol. 463?464, pp. 245–260, 2018.
[26] J. Fridrich, M. Goljan, and R. Du, "Invertible authentication watermark for JPEG images," in *Proc. IEEE International Conference on Information Technology: Coding and Computing*, 2001, pp. 223–227.
[27] ——, "Lossless data embedding for all image formats," in *Proc. SPIE*, 2002, pp. 572–583.
[28] J. Fridrich, M. Goljan, Q. Chen, and V. Pathak, "Lossless data embedding with file size preservation," in *Proc. EI SPIE Security and Watermarking of Multimedia Contents VI*, vol. 5306, 2004, pp. 354–365.
[29] M. Iwata, K. Miyake, and A. Shiozaki, "Digital steganography utilizing features of JPEG images," *IEICE Transactions on Fundamentals*, vol. E87-A, no. 4, pp. 929–936, 2004.
[30] D.-D. Hou, H. Q. Wang, W.-M. Zhang, and N. H. Yu, "Reversible data hiding in JPEG image based DCT frequency and block selection," *Signal Process.*, vol. 177, no. 13, pp. 2768–2786, 2007.
[31] G. Xuan, Y. Q. Shi, Z. Ni, P. Chai, X. Cui, and X. Tong, "Reversible data hiding for JPEG images based on histogram pairs," in *Proc. Int. Conf. Image Anal. Recognit., Montreal, QC, Canada*, 2007, pp. 715–727.
[32] B. G. Mobasseri, R. Berger, M. P. Marcinak, and Y. NaikRaikar, "Data embedding in JPEG bitstream by code mapping," *IEEE Transactions on Image Processing*, vol. 19, no. 4, pp. 958–966, 2010.
[33] Z. Qian and X. Zhang, "Lossless data hiding in JPEG bitstream," *J. Syst. Softw.*, vol. 85, no. 2, pp. 309–313, 2012.
[34] Y. J. Hu, K. Wang, and Z.-M. Lu, "An improved vlc-based lossless data hiding scheme for JPEG images," *J. Syst. Softw.*, vol. 86, pp. 2166–2173, 2013.
[35] K. Wang, Z.-M. Lu, and Y.-J. Hu, "A high capacity lossless data hiding scheme for JPEG images," *J. Syst. Softw.*, vol. 86, pp. 1965–1975, 2013.
[36] S. A. Parah, J. A. Sheikh, N. A. Loan, and G. M. Bhat, "Robust and blind watermarking technique in DCT domain using inter-block coefficient differencing," *Digit. Signal Process.*, vol. 53, pp. 11–24, 2016.
[37] F. J. Huang, X. C. Qu, H. J. Kim, and J. W. Huang, "Reversible data hiding in JPEG images," *IEEE Trans. Circuits Syst. Video Technol.*, vol. 26, no. 9, pp. 1610–1621, 2015.
[38] N. Li and F. J. Huang, "Reversible data hiding for JPEG images based on pairwise nonzero AC coefficient expansion," *Signal Process.*, vol. 171, pp. 1–8, 2013.
[39] J. H. He, J. X. Chen, and S. H. Tang, "Reversible data hiding in JPEG images based on negative influence models," *IEEE Trans. Inf. Forensics Secur.*, vol. 15, pp. 2121–2133, 2020.
[40] J. H. He, J. X. Chen, W. Q. Luo, S. H. Tang, and J. W. Huang, "A novel high-capacity reversible data hiding scheme for encrypted JPEG bitstreams," *IEEE Trans. Circuits Syst. Video Technol.*, vol. 29, no. 12, pp. 3501–3515, 2020.
[41] Z. X. Qian, H. S. Xu, X. Y. Luo, and X. P. Zhang, "New framework of reversible data hiding in encrypted JPEG bitstreams," *IEEE Trans. Circuits Syst. Video Technol.*, vol. 29, no. 2, pp. 351–362, 2020.
[42] W. Hong, Y. Ma, H. C. Wu, and T. S. Chen, "An efficient reversible data hiding method for AMBTC compressed images," *Multimed. Tools Appl.*, vol. 76, no. 4, pp. 5441–5460, 2016.
[43] C. C. Chang, T. S. Chen, Y. Wang, and Y. Liu, "A reversible data hiding scheme based on absolute moment block truncation coding compression using exclusive or operator," *Multimedia Tools Appl.*, vol. 77, pp. 9039–9053, 2018.
[44] W. Hong, X. Y. Zhou, and D.-C. Lou, "A recoverable ambtc authentication scheme using similarity embedding strategy," *PLOS ONE*, pp. 1–19, 2019.
[45] D. Ou and W. Sun, "High payload image steganography with minimum distortion based on absolute moment block truncation coding," *Multimed Tools Appl.*, vol. 74, no. 21, pp. 9117–9139, 2015.
[46] W. Sun, Z. M. Lu, Y. C.Wen, F. X. Yu, and R. J. Shen, "High performance reversible data hiding for block truncation coding compressed images," *Signal, Image Video Process.*, vol. 7, pp. 297–306, 2013.

[47] W. Hong, X. Y. Zhou, and S. W. Weng, "Joint adaptive coding and reversible data hiding for ambtc compressed images," *Symmetry*, vol. 10, no. 7, pp. 254–267, 2018.
[48] W. B. Zheng, C.-C. Chang, and S. W. Weng, "A novel adjustable rdh method for ambtc-compressed codesusing one-to-many map," *IEEE Access*, vol. 8, pp. 13 105–13 118, 2020.
[49] X. Zhang, "Reversible data hiding in encrypted image," *IEEE Signal Process. Lett.*, vol. 18, no. 4, pp. 255–258, 2011.
[50] W. Hong, T.-S. Chen, and H.-Y. Wu, "An improved reversible data hiding in encrypted images using side match," *IEEE Signal Process. Lett.*, vol. 19, no. 4, pp. 199–202, 2012.
[51] C. Qin, W. Zhang, F. Cao, X. P. Zhang, and C. C. Chang, "Separable reversible data hiding in encrypted images via adaptive embedding strategy with block selection," *Signal Process.*, vol. 153, pp. 109–122, 2018.
[52] Z. L. Liu and C. M. Pun, "Reversible data-hiding in encrypted images by redundant space transfer," *Inf. Sci.*, vol. 433?434, pp. 188–203, 2018.
[53] C. Qin, X. Qian, W. Hong, and X. Zhang, "An efficient coding scheme for reversible data hiding in encrypted image with redundancy transfer," *Inf. Sci.*, vol. 487, pp. 176–192, 2019.
[54] L. Ming, X. Di, Y. Zhang, and N. Hai, "Reversible data hiding in encrypted images using cross division and additive homomorphism," *Signal Process.: Image Commun.*, vol. 39, no. PA, pp. 234–248, 2015.
[55] K. Ma, W. Zhang, X. Zhao, N. Yu, and F. Li, "Reversible data hiding in encrypted images by reserving room before encryption," *IEEE Trans. Inform. Forensics Secur.*, vol. 8, no. 3, pp. 553–562, 2013.
[56] W. Zhang, K. Ma, and N. Yu, "Reversibility improved data hiding in encrypted images," *Signal Process.*, vol. 94, no. 1, pp. 118–127, 2014.
[57] S. Yi and Y. Zhou, "Binary-block embedding for reversible data hiding in encrypted images," *Signal Process.*, vol. 133, pp. 40–51, 2017.
[58] C. Qin, Z. H. He, X. Y. Luo, and J. Dong, "Reversible data hiding in encrypted image with separable capability and high embedding capacity," *Inf. Sci.*, vol. 465, pp. 285–304, 2018.
[59] K. Chen and C. Chang, "High-capacity reversible data hiding in encrypted images based on extended run-length coding and block-based msb plane rearrangement," *J. Vis. Commun. Image Represent.*, vol. 58, pp. 334–344, 2019.
[60] S. Xiang and X. Luo, "Reversible data hiding in homomorphic encrypted domain by mirroring ciphertext group," *IEEE Trans. Circ. Syst. Video Technol.*, vol. 28, no. 11, pp. 3099–3110, 2018.
[61] Y. C. Chen, C.-W. Shiu, and G. Horng, "Encrypted signal-based reversible data hiding with public key cryptosystem," *J. Vis. Commun. Image Represent.*, vol. 25, no. 5, pp. 1164–1170, 2018.
[62] S. W. Weng, C. Y. Zhang, T. C. Zhang, and K. M. Chen, "High capacity reversible data hiding in encrypted images using SIBRW and GCC," *J. Vis. Commun. Image Represent.*, 2020, DOI: 10.1016/j.jvcir.2020.102932.
[63] C. D. Vleeschouwer, J. Delaigle, and B. Macq, "Circular interpretation of histogram for reversible watermarking," in *Proceedings of the IEEE Workshop on Multimedia Signal Processing*, 2001, pp. 345–350.
[64] ——, "Circular interpretation of bijective transformations in lossless watermarking for media asset management," *IEEE Trans. Multimedia*, vol. 5, no. 1, pp. 97–105, 2003.
[65] Z. Ni, Y. Shi, N. Ansari, W. Su, Q. Sun, and X. Lin, "Robust lossless image data hiding designed for semi-fragile image authentication," *IEEE Trans. Circuits Syst. Video Technol.*, vol. 18, no. 4, pp. 497–509, 2008.
[66] X.-T. Zeng, L.-D. Ping, and X.-Z. Pan, "A lossless robust data hiding scheme," *Pattern Recognit.*, vol. 43, no. 4, pp. 1656–1667, 2010.
[67] X. Gao, L. An, Y. Yuan, D. Tao, and X. Li, "Lossless data embedding using generalized statistical quantity histogram," *IEEE Trans. Circuits Syst. Video Technol.*, vol. 21, no. 8, pp. 1061–1070, 2011.
[68] L. An, X. Gao, X. Li, D. Taoa, C. Deng, and J. Li, "Robust reversible watermarking via clustering and enhanced pixel-wise masking," *IEEE Trans. Image Process.*, vol. 21, no. 8, pp. 3598–3611, 2012.
[69] L. An, X. Gao, Y. Yuan, and D. Tao, "Robust lossless data hiding using clustering and statistical quantity histogram," *Neurocomputing*, vol. 77, no. 1, pp. 1–11, 2012.
[70] L. An, X. Gao, Y. Yuan, D. Tao, C. Deng, and F. Ji, "Content-adaptive reliable robust lossless data embedding," *Neurocomputing*, vol. 79, pp. 1–11, 2012.

[71] R. Thabit and B. E. Khoo, "Robust reversible watermarking scheme using slantlettransform matrix," *J. Syst. Software*, vol. 88, pp. 74–86, 2014.
[72] X. Wang, X. L. Li, and Q. Q. Pei, "Independent embedding domain based two-stage robust reversible watermarking," *IEEE Trans. Circuits Syst. Video Technol.*, vol. 30, no. 8, pp. 2406–2417, 2012.
[73] Z. M. Lu, H. Luo, and J.-S. Pan, "Reversible watermarking for error diffused halftone image using statistical features," *Lecture Notes in Computer Science*, vol. 4283, pp. 71–81, 2006.
[74] J. S. Pan, H. Luo, and Z. M. Lu, "A lossless watermarking scheme for halftone image authentication," in *International Journal of Computer Science and Network Security*, vol. 6, no. 2B, 2006, pp. 147–151.
[75] P. S. Liao, J. S. Pan, Y. H. Chen, and B. Y. Liao, "A lossless watermarking technique for halftone images," in *International Workshop on Intelligent Information Hiding and Multimedia Signal Processing*, no. LNAI 3682, 2005, pp. 593–599.
[76] D. W. Xu, R. D. Wang, and Y. Q. Shi, "An improved reversible data hiding-based approach for intra-frame error concealment in H.264/AVC," *J. Vis. Commun. Image R.*, vol. 25, pp. 410–422, 2014.
[77] G. Song, Z. Li, J. Zhao, J. Hu, and H. Tu, "A reversible video steganography algorithm for MVC based on motion vector," *Multimedia Tools Appl.*, vol. 74, no. 11, pp. 3759–3782, 2015.
[78] J. Zhao, Z.-T. Li, and B. Feng, "A novel two-dimensional histogram modication for reversible data embedding into stereo H.264 video," *Multimedia Tools Appl.*, vol. 75, no. 10, pp. 5959–5980, 2016.
[79] D. W. Xu and R. D. Wang, "Two-dimensional reversible data hiding-based approach for intra-frame error concealment in h.264/avc," *Signal Process.: Image Commun.*, vol. 47, pp. 369–379, 2016.
[80] Y. X. Liu, L. Chen, M. S. Hu, Z. J. Jia, S. M. Jia, and H. G. Zhao, "A reversible data hiding method for H.264 with shamir's (t, n)-threshold secret sharing," *Neurocomputing*, vol. 188, no. 5, pp. 63–70, 2016.
[81] K.-L. Chung, C.-Y. Chiu, T.-Y. Yu, and P.-L. Huang, "Temporal and spatial correlation-based reversible data hiding for RGB CFA videos," *Inf. Sci.*, vol. 420, pp. 386–402, 2017.
[82] D. Xu and R. Wang, "Effcient reversible data hiding in encrypted H.264/AVC videos," *J. Electron. Imag.*, vol. 23, no. 5, pp. 1–14, 2014.
[83] Y. Z. Yao, W. M. Zhang, and N. H. Yu, "Inter-frame distortion drift analysis for reversible data hiding in encrypted H.264/AVC video bitstreams," *Signal Process.*, vol. 128, pp. 531–545, 2016.
[84] D. Yan and R. Wang, "Reversible data hiding for audio based on prediction error expansion," in *Proc. Int. Conf. Intell. Inf. Hiding Multimedia Signal Process.*, 2008, pp. 249–252.
[85] A. Nishimura, "Reversible audio data hiding using linear prediction and error expansion," in *Proc. Int. Conf. Intell. Inf. Hiding Multimedia Signal Process.*, 2011, pp. 318–321.
[86] F. Wang, Z. Xie, and Z. Chen, "High capacity reversiblewatermarking for audio by histogram shifting and predicted error expansion," *Sci. World J.*, vol. 2014, no. 656251, 2014.
[87] A. Nishimura, "Reversible audio data hiding based on variable error expansion of linear prediction for segmental audio and g.711 speech," *IEICE Trans. Inf. Syst.*, vol. 99-D, no. 1, pp. 83–91, 2016.
[88] X. L. Q. Chen, S. Xiang, "Reversible watermarking for audio authentication based on integer DCT and expansion embedding," in *International Workshop on Digital Watermarking*, 2012, pp. 224–239.
[89] M. Y. Li, Y. H. Jiao, and X. N. Niu, "Reversible watermarking for compressed speech," in *2008 Eighth International Conference on Intelligent Systems Design and Applications*, 2008, pp. 197–201.
[90] S. W. Weng, Y. Zhao, J. S. Pan, and R. R. Ni, "Reversible watermarking based on invariability and adjustment on pixel pairs," *IEEE Signal Process. Lett.*, vol. 45, no. 20, pp. 1022–1023, 2008.
[91] X. Wang, X. L. Li, and B. Yang, "High capacity reversible image watermarking based on integer transform," in *Proceedings of ICIP*, 2010, pp. 217–220.
[92] X. Wang, X. L. Li, B. Yang, and Z. M. Guo, "Efficient generalized integer transform for reversible watermarking," *IEEE Signal Process. Lett.*, vol. 17, no. 6, pp. 567–570, 2010.
[93] F. Peng, X. Li, and B. Yang, "Adaptive reversible data hiding scheme based on integer transform," *Signal Process.*, vol. 92, no. 1, pp. 54–62, 2012.
[94] S. W. Weng and J.-S. Pan, "Integer transform based reversible watermarking incorporating block selection," *J. Vis. Commun. Image Represent.*, vol. 35, pp. 25–35, 2016.
[95] C. Qin and X. P. Zhang, "Effective reversible data hiding in encrypted image with privacy protection for image content," *J. Vis. Commun. Image R.*, vol. 31, pp. 154–164, 2015.
[96] W. Hong, T. S. Chen, and C. W. Shiu, "Reversible data hiding for high quality images using modification of prediction errors," *J. Syst. Software*, vol. 82, no. 11, pp. 1833–1842, 2009.

[97] C. F. Lee, H. L. Chen, and H. K. Tso, "Embedding capacity raising in reversible data hiding based on prediction of difference expansion," *J. Syst. Software*, vol. 83, no. 10, pp. 1864–1872, 2014.
[98] X. L. Li, B. Yang, and T. Y. Zeng, "Efficient reversible watermarking based on adaptive prediction-error expansion and pixel selection," *IEEE Trans. Image Process.*, vol. 20, no. 12, pp. 3524–3533, 2011.
[99] W. Hong and T. S. Chen, "Reversible data embedding for high quality images using interpolation and reference pixel distribution mechanism," *J. Vis. Commun. Image R.*, vol. 22, no. 2, pp. 131–140, 2011.
[100] C. Qin, C. C. Chang, Y. H. Huang, and L. T. Liao, "An inpainting-assisted reversible steganographic scheme using a histogram shifting mechanism," *IEEE Trans. Circ. Syst. Video Technol.*, vol. 23, no. 7, pp. 1109–1118, 2013.
[101] G. R. Feng and L. Y. Fan, "Reversible data hiding of high payload using local edge sensing prediction," *J. Syst. Software*, vol. 85, no. 2, pp. 392–399, 2012.
[102] T. C. Lu, C. Y. Tseng, and K. M. Deng, "Reversible data hiding using local edge sensing prediction methods and adaptive thresholds," *Signal Process.*, vol. 104, pp. 152–166, 2014.
[103] Q. Li, B. Yan, H. Li, and J. S. Pan, "Reversible watermarking based on adaptive prediction error expansion," in *International Conference on Genetic and Evolutionary Computing*, 2018, pp. 243–251.
[104] B. Ou, X. L. Li, Y. Zhao, and R. R. Ni, "Reversible data hiding using invariant pixel-value-ordering and prediction-error expansion," *Signal Process.: Image Commun.*, vol. 29, no. 7, pp. 198–205, 2014.
[105] X. C. Qu and H. J. Kim, "Pixel-based pixel value ordering predictor for high-fidelity reversible data hiding," *Signal Process.*, vol. 111, pp. 249–260, 2015.
[106] S. W. Weng, G. H. Zhang, J.-S. Pan, and Z. L. Zhou, "Optimal ppvo-based reversible data hiding," *J. Vis. Commun. Image Represent.*, vol. 48, pp. 317–328, 2017.
[107] F. Peng, X. L. Li, and B. Yang, "Improved pvo-based reversible data hiding," *Digit. Signal Process.*, vol. 25, pp. 255–265, 2014.
[108] W. Hong, M. J. Chen, and T. S. Chen, "An efficient reversible image authentication method using improved PVO and LSB substitution techniques," *Signal Process.: Image Commun.*, vol. 58, pp. 111–122, 2017.
[109] S. W. Weng, J.-S. Pan, and L. D. Li, "Reversible data hiding based on an adaptive pixel-embedding strategy and two-layer embedding," *Inf. Sci.*, vol. 369, pp. 144–159, 2016.
[110] S. W. Weng, Y. Q. Shi, W. Hong, and Y. Yao, "Dynamic improved pixel ordering reversible data hiding," *Inf. Sci.*, vol. 489, pp. 136–154, 2019.
[111] X. Wang, J. Ding, and Q. Q. Pei, "A novel reversible image data hiding scheme based on pixel value ordering and dynamic pixel block partition," *Inf. Sci.*, vol. 310, pp. 16–35, 2015.
[112] S. W. Weng, Y. J. Liu, J.-S. Pan, and N. Cai, "Reversible data hiding based on flexible block-partition and adaptive block-modification strategy," *J. Vis. Commun. Image Represent.*, vol. 41, pp. 185–199, 2016.
[113] B. Ou, X. L. Li, Y.Zhao, R. R. Ni, and Y. Q. Shi, "Pairwise prediction-error expansion for efficient reversible data hiding," *IEEE Trans. Image Process.*, vol. 22, no. 8, pp. 5010–5021, 2013.
[114] I.-C. Dragoi and D. Coltuc, "Adaptive pairing reversible watermarking," *IEEE Trans. Image Process.*, vol. 25, no. 5, pp. 2420–2422, 2016.
[115] B. Ou, X. L. Li, W. M. Zhang, and Y. Zhao, "Improving pairwise pee via hybrid-dimensional histogram generation and adaptive mapping selection," *IEEE Trans. Circuits Syst. Video Technol.*, vol. 29, no. 7, pp. 2176–2190, 2019.
[116] B. Ou, X. L. Li, and J. W. Wang, "High-fidelity reversible data hiding based on pixel-value-ordering and pairwise prediction-error expansion," *J. Vis. Commun. Image R.*, vol. 39, pp. 12–23, 2016.
[117] W. G. He, G. Q. Xiong, S. W. Weng, Z. C. Cai, and Y. M. Wang, "Reversible data hiding using multi-pass pixel-value-ordering and pairwise prediction-error expansion," *Inf. Sci.*, vol. 467, pp. 784–799, 2018.
[118] M. Y. Xiao, X. L. Li, Y. Y. Wang, Y. Zhao, and R. R. Ni, "Reversible data hiding based on pairwise embedding and optimal expansion path," *Signal Process.*, vol. 158, pp. 210–218, 2019.
[119] J. Li, X. L. Li, B. Yang, and X. M. Sun, "Segmentation-based image copy-move forgery detection scheme," *IEEE Trans. Inf. Forensic Secur.*, vol. 10, no. 3, pp. 507–518, 2015.
[120] J. X. Wang, N. X. Mao, X. Chen, J. Q. Ni, and Y. Q. Shi, "Multiple histograms based reversible data hiding by using fcm clustering," *Signal Processing*, vol. 159, pp. 193–203, 2019.
[121] H. Yao, F. Mao, T. Tang, and C. Qin, "High-fidelity dual-image reversible data hiding via prediction-error," *Signal Process.*, vol. 170, pp. 1–13, 2020.

[122] H. Yao, H. Wei, C. Qin, and Z. Tang, "A real-time reversible image authentication method using uniform embedding strategy," *Journal of Real-Time Image Process.*, vol. 17, no. 1, pp. 41–54, 2020.
[123] S. W. Weng, W. L. Tan, B. Ou, and J.-S. Pan, "Reversible data hiding method for multi-histogram point selection based on improved crisscross optimization algorithm," *Inf. Sci.*, vol. 549, pp. 13–33, 2021.
[124] H. S. Chen, J. Q. Ni, W. Hong, and T.-S. Chen, "Reversible data hiding with contrast enhancement using adaptive histogram shifting and pixel value ordering," *Signal Process.: Image Commun.*, vol. 16, pp. 1–16, 2016.
[125] H. T. Wu, J.-L.Dugelay, and Y.-Q. Shi, "Reversible image data hiding with contrast enhancement," *IEEE Signal Process. Lett.*, vol. 22, no. 1, pp. 81–85, 2015.
[126] H. T. Wu, J. W. Huang, and Y.-Q. Shi, "A reversible data hiding method with contrast enhancement for medical images," *J. Vis. Commun. Image Represent.*, vol. 31, pp. 146–153, 2015.
[127] H. T. Wu, S. H. Tang, J. W. Huang, and Y. Q. Shi, "A novel reversible data hiding method with image contrast enhancement," *Signal Process.: Image Commun.*, vol. 62, pp. 64–73, 2018.
[128] G. Y. Gao and Y.-Q. Shi, "Reversible data hiding using controlled contrast enhancement and integer wavelet transform," *IEEE Signal Process. Lett.*, vol. 22, no. 11, pp. 2078–2082, 2015.
[129] I. F. Jafar, K. A. Darabkh, and R. R. Saifan, "Sardh: A novel sharpening-aware reversible data hiding algorithm," *J. Vis. Commun. Image R.*, vol. 39, no. 8, pp. 239–252, 2016.
[130] G. Y. Gao, X. D. Wan, S. M. Yao, Z. M. Cui, C. X. Zhou, and X. M. Sun, "Reversible data hiding with contrast enhancement and tamper localization for medical images," *Inf. Sci.*, vol. 385-386, pp. 250–265, 2017.
[131] S. W. Weng, Y. J. Liu, Y. Q. Shi, B. Ou, C. Y. Zhang, and C. P. Wang, "A general framework of reversible data hiding with controlled contrast enhancement," *Computers, Materials & Continua*, vol. 62, no. 1, pp. 157–177, 2020.
[132] M. Lema and O. Mitchell, "Absolute moment block truncation coding and its application to color image," *IEEE Trans. Commun.*, vol. 29, no. 7, pp. 198–205, 1984.
[133] D. Coltuc, "Towards distortion-free robust image authentication," *Journal of Physics: Conference Series*, vol. 77, pp. 1–7, 2007.
[134] D. Coltuc and J.-M. Chassery, "Towards distortion-free robust image authentication," in *Electronic Imaging 2007, International Society for Optics and Photonics*, vol. 77, 2007, pp. 65 051N–65 051N.
[135] Y. Q. Shi, X. L. Li, X. P. Zhang, H. T. Wu, and B. Ma, "Reversible data hiding: Advances in the past two decades," *IEEE Access*, vol. 4, pp. 3210–3237, 2016.